Nanoscale

PAPER

Angular dependence of the magnetoresistance effect in a silicon based p–n junction device†

Cite this: *Nanoscale*, 2014, **6**, 3978

Tao Wang,[a] Mingsu Si,[a] Dezheng Yang,*[a] Zhong Shi,[b] Fangcong Wang,[a] Zhaolong Yang,[a] Shiming Zhou[b] and Desheng Xue*[a]

Received 9th August 2013
Accepted 2nd January 2014

DOI: 10.1039/c3nr04077a

www.rsc.org/nanoscale

We report a pronounced angular dependence of the magnetoresistance (MR) effect in a silicon based p–n junction device at room temperature by manipulating the space charge region of the p–n junction under a magnetic field. For the p–n junction device with various space charge region configurations, we find that all the angular dependence of the MR effect is proportional to $\sin^2(\theta)$, where the θ is the angle between the magnetic field and the driving current. With increasing the magnetic field and driving current, the anisotropic MR effect is obviously improved. At room temperature, under a magnetic field 2 T and driving current 20 mA, the MR ratio is about 50%, almost one order of amplitude larger than that in the magnetic material permalloy. Our results reveal an interpretation of the MR effect in the non-magnetic p–n junction in terms of the Lorentz force and give a new way for the development of future magnetic sensors with non-magnetic p–n junctions.

1 Introduction

The control and manipulation of the electron charge and spin by a magnetic field in semiconductor electronic devices are central aspects of spintronics.[1] This will have a profound impact on existing and emerging semiconductor industries. Recently such magnetic field-controlled semiconductor electronics have become possible by utilizing the large MR effect in non-magnetic semiconductor materials, such as AgAs,[2,3] GaAs,[4] InSb,[5] *etc.*, which combines the traditional electronic technology with current magnetronic technology naturally.

From the application view of point, silicon can be considered as an ideal magnetic field-controlled semiconductor material, because it is fully compatible with the current CMOS technology and long spin coherence, as well as being low-cost.[6] Despite of the low carrier mobility in silicon, the MR ratio in silicon at room temperature has still been reported to be much larger than that in magnetic materials, by tunneling injection,[7,8] inhomogeneity scattering,[9,10] density fluctuation[12] and current jetting.[12] In contrast with the MR effect in magnetic materials that results from the spin-dependent transport of carriers,[13] this large MR effect in silicon is derived from the deformation of current paths in inhomogeneous conductors. This causes an uncompensated Hall field to be involved in the transverse MR effect.[14–19]

As an extension of the single doped silicon material with a large MR effect, the p–n junction device based on silicon is an excellent platform for future magneto-electronics in the semiconductor industry. This is because the p–n junction structure can be considered as a typical electron and hole coexistence system. Due to the opposite sign of the carrier mobility between the electron and the hole, the fluctuation of the carrier mobility in the p–n junction becomes very large and subsequently enhances the MR effect significantly.[14,15] Although the geometry-enhanced MR might be caused by the measurement method,[11,20] we also note that a p–n boundary could still enhance MR in certain circumstances according to theoretical calculations and experiments by ourselves and others.[19,21] More importantly, an intrinsic space charge region in the p–n junction can be formed at the interface between the p and n semiconductors. One possible way to enhance the magnetotransport properties is to design and manipulate the intrinsic space charge region of the p–n junction under a magnetic field. In our previous work, we have shown that control of the space charge region configurations by magnetic field, instead of external electric field, can efficiently affect the transport properties in the p–n junction.[21] Owing to the intrinsic space charge region, the large MR effect in the p–n junction has a small driving voltage only 6 V, while in the doped silicon a large voltage 60 V should

[a]*The Key Laboratory for Magnetism and Magnetic materials of Ministry of Education, Lanzhou University, Lanzhou 730000, China. E-mail: yangdzh@lzu.edu.cn; xueds@lzu.edu.cn*

[b]*The Department of physics, Tongji University, Shanghai 200092, China*

† Electronic supplementary information (ESI) available: S1(a) shows the *I–V* characteristics of the p–n junction device for various magnetic field orientations in the *x–z* plane at room temperature. S1(b) shows the corresponding anisotropic MR curves at specific current $I = 20$ mA. S2 shows the *I–V* characteristics of the p–n junction device while the magnetic field is applied in the *x–y* plane. S3 shows the *I–V* curves at negative bias with various magnetic fields. S4(a) shows the *I–V* curves of the sample in various electrodes without a magnetic field. The size of the sample is 2.9 mm × 2.26 mm, and the thickness is 0.14 mm. S4(b) shows the Hall voltage in the sample's n region for the current $I = 0.01$ mA. See DOI: 10.1039/c3nr04077a

be provided to observe an appreciable MR effect. Furthermore, the p–n junctions are fundamental elements in modern semiconductors, so the large MR effect in the p–n junction can be more easily integrated into modern semiconductor electronics. Very recently, by utilizing the InSb p–n junctions with large MR effect, magnetic-field-controlled reconfigurable semiconductor logic has been proposed and demonstrated, which indicates a new kind of spintronic device based on a non-magnetic semiconductor.[22]

However, until now few experiments have been found to systematically study the angular dependence of these magnetotransport characteristics of non-magnetic semiconductors. The lack of such a magnetic field orientation to control MR effects significantly limits the applications of non-magnetic materials. Moreover, the anisotropic magnetotransport properties of non-magnetic semiconductors can help us further understand the mechanism of these unusual MR properties of the p–n junction.

In this work, we investigate the angular dependence of the magnetotransport characteristics in a silicon based p–n junction device with various space charge region configurations. A pronounced anisotropic MR effect in the silicon based p–n junction device, one or two orders of amplitude larger than that in a magnetic material, is observed at room temperature. Interestingly, the detailed dependence of the p–n junction resistance on the angle θ between the direction of the current and the magnetic field can be fitted well with a $\sin^2(\theta)$ relationship. This is also the same angular dependence observed in magnetic materials, *e.g.* permalloy, despite the fact that the mechanisms behind them are completely different. These results are promising for the development of the future magnetoelectric devices based on semiconductors.

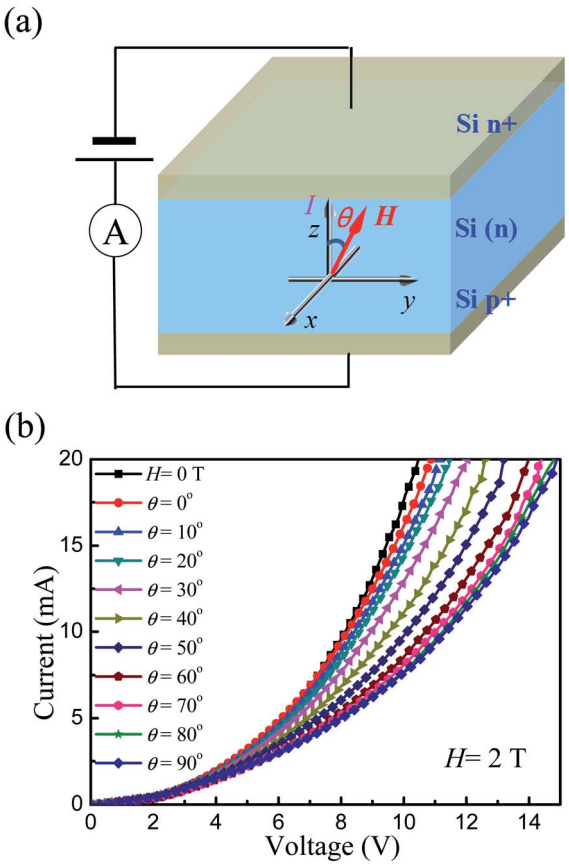

Fig. 1 (a) Schematic illustration of the p–n junction device structure and measurement sketch. (b) The *I*–*V* characteristics under magnetic field $H = 2$ T at various angles θ from 0° to 90°.

2 Experiment

The samples were fabricated by MEMS (Micro Electro Mechanical Systems). The wafers were lightly doped with a 10^{12} atom cm^{-3} n-type dopant to achieve a good surface resistivity higher than 2000 Ω cm. An oxidation film with a thickness of 6000 Å was grown on the wafers in the oxidation furnace at 1030 °C for 4 hours. After that, the micro-strip patterns were transferred to the wafers by a lithography machine. Then the wafers were further treated with a boron implantation (40 Kev, 2×10^{14} atom cm^{-3}) on the top surface and a phosphorus implantation (60 Kev, 1×10^{15} atom cm^{-3}) at the back surface by a medium-energy ion implanter. Finally the Cu electrodes at the top and bottom were sputtered separately with the high vacuum 3×10^{-5} Pa.

In order to show how the space charge region affects the magnetotransport characteristics in the p–n junction, the voltage between the top and bottom of samples were applied to cause the current I to pass perpendicularly though the space charge region, as shown in Fig. 1a. By rotating the sample holder, the orientation of the magnetic field H applied to the device could be controlled to measure the anisotropic MR effect. The MR ratio was defined as $(\rho_H - \rho_0)/\rho_0$, where ρ_H and ρ_0 are the resistivities with and without the magnetic field, respectively. Here we used the Keithley 2400, 220, and 2000 as the voltage source, the current source and the voltage (current) meter, respectively. For the data in Fig. 1b, S1a, S2a and S3,† we applied the voltage and measured the current under different magnetic fields. For the data in Fig. 3, S1b, S2b and S4b,† we used the current source for a specified current and measured the voltage as a function of the orientation of magnetic field.

3 Results and discussion

Fig. 1a shows the schematic illustration of the p–n junction device structure and the related measurement diagram. In contrast to the magnetodiode with lateral geometry,[23] the structure Si(p+)/Si(n)/Si(n+) with vertical geometry is chosen to form a wide space charge region. At room temperature the carrier densities of Si(p+), Si(n), and Si(n+) were 2.0×10^{14} cm^{-3}, 1.0×10^{12} cm^{-3} and 1.0×10^{15} cm^{-3}, respectively. Thus, the width of the formed space charge region in Si(p+) and Si(n+) is about 100 nm, but the width in Si(n) is 22 μm, which critically depends on the intrinsic competition between the diffusion process and the built-in electric field. The thickness of the n region is about 400 μm.

Fig. 1b shows the typical *I*–*V* characteristics of the p–n junction device for various magnetic field orientations at room temperature. All the *I*–*V* curves exhibit the obvious rectifying

features due to the space charge region formed in the p–n junction. The *I–V* characteristics can be described by the Shockley equation. In contrast, in the reported single doped silicon device the *I–V* characteristics obey Ohm's law at the low electric field and the Mott–Gurney law at the high electric field.[10] However, when the external magnetic field amplitude and orientation are changed, the transport characteristics in the p–n junction is also obviously modulated. In the case of the zero-magnetic field *I–V* curve, the junction current is about 20 mA at $V = 10$ V. As the external magnetic field is applied, a pronounced current suppression effect occurs, and increases with the increase of θ from 0° to 90°. This indicates a large anisotropic MR effect in the p–n junction. Remarkably, one can also find that the anisotropic MR effect strongly depends on the applied current or voltage. The anisotropic MR effect is more significant at the larger current or voltage level. When the applied voltage and the magnetic field are increased to 10 V and 2 T, respectively, the anisotropic MR ratio can reach about 160% at room temperature. We also note that in the single doped silicon at room temperature the MR ratios were above 1000% at 3 T and around 350% at 0.5 T with a large voltage bias of 70 V.[10] Schoonus *et al.* also observed a arge MR effect in single doped silicon at room temperature, in which the highest MR ratio could be reach above 1000% at 1.26 T with a voltage of 80 V.[7] Although the MR ratio in our p–n junction is lower than that of single doped silicon at room temperature, the MR effect of the p–n junction has a small driving voltage (<10 V) owing to the intrinsic space charge region, which is an advantage for future applications.

Below we will analyze the underlying mechanism in Fig. 1. The MR effect in p–n junction in our work is much more complicated than that in the materials worked in the linear transport region.[24] Obviously, the transport characteristics in the p–n junction are dominated by the space–charge distribution. When the width of space charge region is changed by the external electric field, the resistance of the p–n junction can vary over the range of several orders of amplitude, also known as the rectifying effect. Based on the similar mechanism mediated by the electric field, we further consider how the intrinsic space charge region of p–n junction evolves under the external magnetic field. When the magnetic field is applied, the carriers in the n-type and p-type regions are deflected by the Lorentz force and accumulate at the edges of the sample (Fig. 2). As a result, a trapezoidal distribution in the space charge region is formed to balance the Lorentz force. Therefore, similar to the rectifying effect under the electric field, the spatial distribution in the space charge region under the external magnetic field can also drastically affect the junction resistance.[21] According to the classical p–n junction transport equations, the carrier concentrations in such trapezoidal space charge regions have an exponential distribution in order to balance the Lorentz force. In this situation the drift force formed by the carrier concentration gradient compensates the Lorentz force, instead of the Hall voltage in the uniform semiconductor, Although the carrier concentrations are redistributed and show an exponential distribution under the magnetic field, the total numbers of carriers are the same for both the uniform distribution without

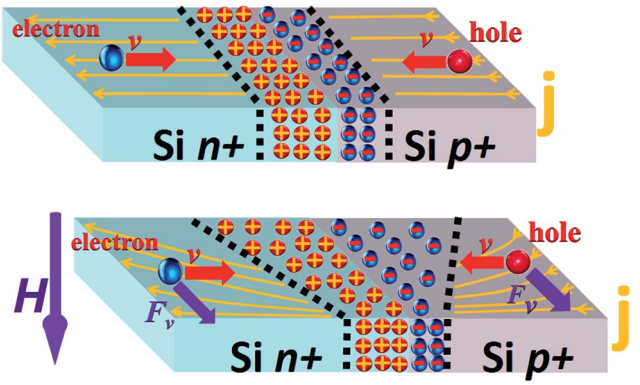

Fig. 2 Schematic illustration of the origin of the large MR effect in the p–n junction due to the spatial modulation of the space charge region induced by the magnetic field. (Top) A uniform distribution in the space charge region is formed when the electronic field is applied. (Bottom) A trapezoidal distribution in the space charge region is formed due to the Lorenz force when the magnetic field is applied. The carriers are deflected due to the space charge region geometry variations.

the magnetic field and the trapezoidal distribution with the magnetic field. In order to keep the total number of carriers conserved, this means that the diffusion barrier in some part of the device is lowered while in another part it is raised. However, considering the exponential distribution of the carrier concentrations, one can easily see that the raised parts of space charge region are one or two orders of amplitude larger than the lowered part. As a result, the total resistance of the p–n junction still increases based on the calculation. This is also consistent with our results.

Obviously, the mechanism in our p–n junction device contrasts to that in previous magnetodiodes with a similar p(+)–n–n(+) structure.[23] The MR effect in previous magnetodiodes results from the magnetic control of the carrier concentration gradient due to the different recombining surfaces and shape ratios. As a result, the corresponding MR ratio behaves in a distinct manner with respect to the sign of applied magnetic field. Here the large MR effect of the p–n junction which is due to the space charge region geometry variation can be ascribed to three possible mechanisms. The first is due to the p–n junction barrier change, where the magnetic field controls the MR effect *via* changing the tunnel carrier concentrations through the p–n junction. The second is that the so-called current trajectory deflected (or current jetting effect) due to the space charge region geometry variation in the p–n junction. This mechanism directly involves the Hall voltage in the transverse MR effect. Interestingly, due to the space charge region geometry, the Hall effect here is uncompensated and could be adjusted with the deformation of space charge region. The final possible mechanism is that the p–n junction can be considered as an electron and hole coexistence model, proposed by Parish and Littlewood, where the MR effect of the p–n junction critically depends on the carrier mobility fluctuations due to the inverse carrier mobility between the electron and hole carriers.[14,15] Because the current level in the p–n junction is directly related to the space charge region, we could measure the anisotropic MR effect *via*

setting the different current levels to represent the various space charge region configurations in the p–n junction device.

The corresponding anisotropic MR curves at specific current levels are presented in Fig. 3. The measured MR voltages for various current levels show a strong anisotropy with two-fold symmetry at room temperature. The minimum value is found both at 0° and 180°, where the magnetic field is parallel to the current, while the maximum value is found at 90° and 270°, where the magnetic field is perpendicular to the current. Interestingly, for various space charge regions by setting different current levels, the voltage as a function of angle θ can be fitted well by the equation

$$V = V_0(I, H) + \Delta V(I, H) \times \sin^2(\theta), \quad (1)$$

where the fitted parameters V_0 and ΔV depend on the applied current I and the magnetic field H. The fitted results are shown as the solid lines in Fig. 3. Again, the anisotropic MR effect is obviously improved with increasing the applied current level, demonstrating that the MR ratio is more sensitive to the magnetic field in the narrower space charge region. We also measured the I–V curves at a negative bias, but no obvious MR effect was observed at the negative bias, which is consistent with the conclusion at the positive bias, as shown in Fig. S3.† However, we also note that for the single doped silicon the MR properties are symmetric at both positive and negative bias.[7–10,12]

In order to further confirm the anisotropic MR of the p–n junction, we measured the angular dependence of the MR curves with magnetic field varied over the range of 0.25 T to 2 T at a fixed current level. As shown in Fig. 4, the anisotropic MR effect drastically decreases as the magnetic amplitude decreases at a fixed current level. However, for different magnetic field amplitudes, all the anisotropic MR curves still fit eqn (1) well, as shown in Fig. 4. This indicates the magnetic field induced anisotropic MR effect over a wide range of current level and

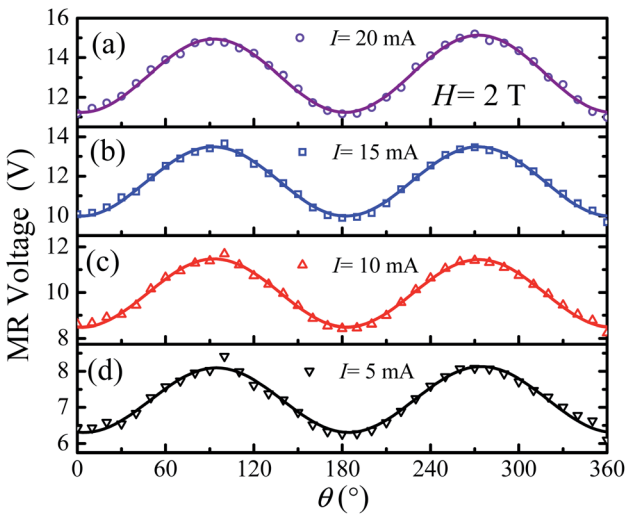

Fig. 3 The angular dependence of the measured MR voltage at specific currents (a) 20 mA, (b) 15 mA, (c) 10 mA and (d) 5 mA with magnetic field $H = 2$ T. The anisotropic MR curves fitted with the $\sin^2(\theta)$ are shown by the solid lines.

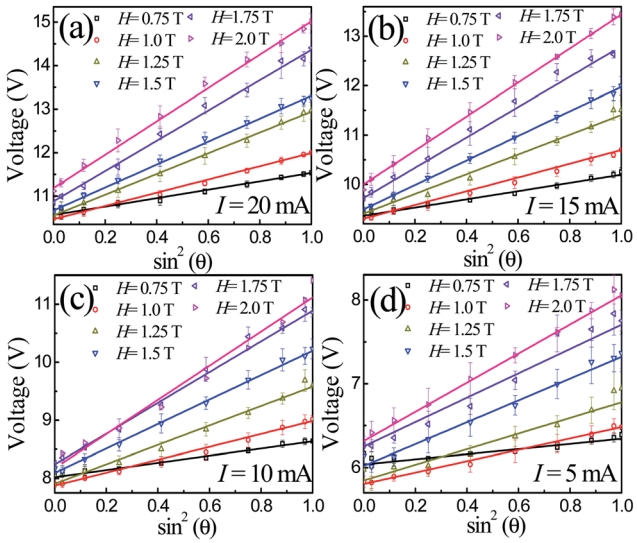

Fig. 4 Angular dependence of the measured MR voltage over a wide magnetic field range at a specific current (a) 20 mA, (b) 15 mA, (c) 10 mA, (d) 5 mA. The lines are fitted by eqn (1).

magnetic field stems from the unified mechanism. The variation in the space charge region as manipulated by the current and magnetic field only affects the fitted parameter values in eqn (1). We also observed an angularly independent MR as noted in Fig. 4. The angularly independent MR effect might stem from the defects, dislocations or electrical inhomogeneities that scatter the carriers.

Although the anisotropic MR behavior in the p–n junction has a similar relationship to that usually observed in ferromagnetic materials, the mechanisms behind them are totally different. The anisotropic MR effect in a ferromagnet is due to the intrinsically anisotropic spin-orbit coupling of conduction electrons. However, the silicon based p–n junction contains no magnetic moments, a spin-mediated mechanism seems unlikely. Furthermore, at room temperature for magnetic field 2 T and current 20 mA, the anisotropic MR ratio of the p–n junction in our work is about 50%, which is almost one order of magnitude larger than that of permalloy. Obviously, the anisotropic MR effect of the p–n junction follows the angular dependence of the Lorentz force acting on the carriers. The behavior that the MR ratio is proportional to $H^2\sin^2(\theta)$ here can be usually understood by the second-order magnetic deflection effect, in which the drift current I_z is deflected twice ($I_z \rightarrow I_x \rightarrow I_z$) due to the Lorentz effect by H_y. This is because the energy of the carriers in the semiconductor is dispersive, and the Hall electric field can not completely cancel the deflection of the carriers, thus inducing a positive MR effect. However, such a MR ratio in silicon is usually two orders of magnitude lower than that reported in the silicon-based p–n junction due to the low carrier mobility of silicon. Here the large anisotropic MR ratio in the silicon based p–n junction mainly stems from the amplification effect by the change of the space charge region under the magnetic field. This asymmetry distribution of the space charge region, which is indicated by the different energy

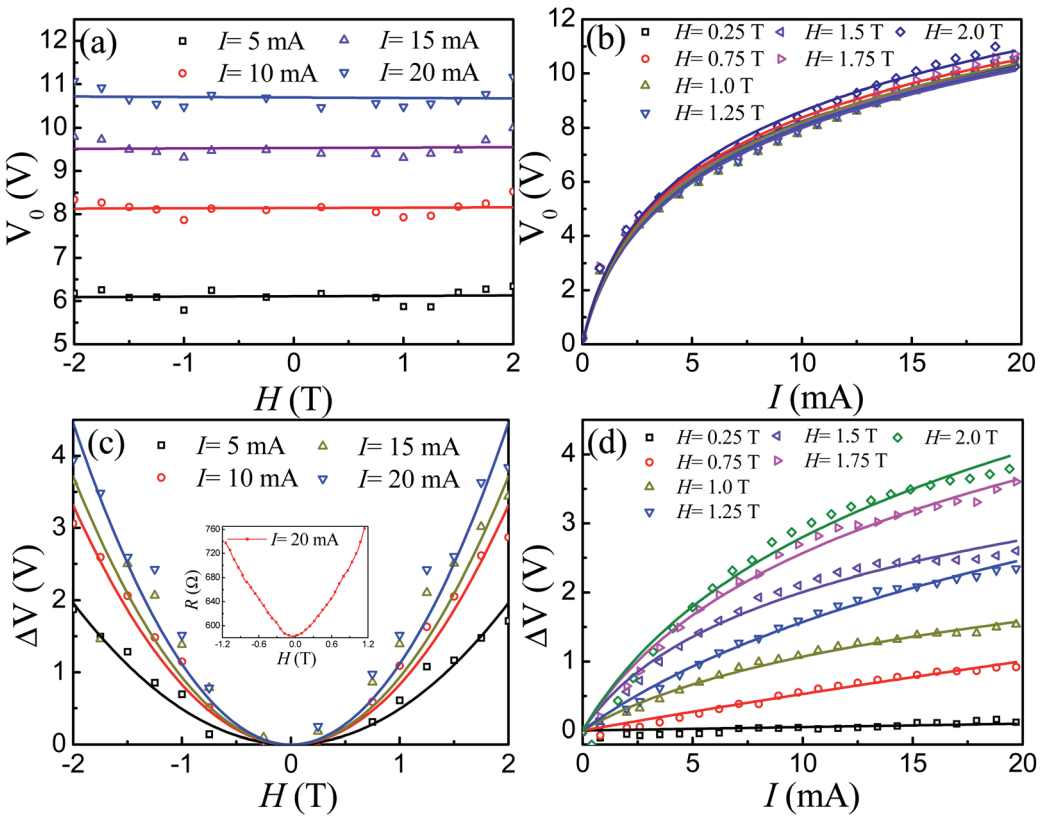

Fig. 5 (a) V_0 as a function of magnetic field H at various currents from 5 mA to 20 mA. (b) V_0 as a function of current I at various H from 0.25 T to 2 T. The solid lines were fitted by the Shockley equation. (c) ΔV as a function of magnetic field H at various currents from 5 mA to 20 mA. The solid lines were fitted by a parabola. Inset shows the typical MR curve at $I = 20$ mA. (d) ΔV as a function of current I at various H from 0.25 T to 2 T. The solid lines were fitted by the Shockley equation.

barrier distributions, can significantly enhance the current deflection toward the lower energy barrier. As a result, similar to the geometry MR effect induced by the sample shape ratio, the MR effect in the p–n junction is directly related to the geometry of the space charge region induced by the magnetic field.

It is also very important and necessary to compare our MR devices with the reported dilute magnetic semiconductors.[25–27] Indeed, a large MR effect at room temperature was also observed in p–(In, Mn)As/n–InAs heterojunctions. Although it has a similar p–n junction structure, the origin of the MR effect differs from that of the silicon-based p–n junction here. For the diluted magnetic semiconductors the large MR effect is still obviously observed even if the magnetic field is applied parallel to the flow of current.[25] More importantly, for non-magnetic InAs p–n junctions (without the Mn doping), the MR ratios at both 78 and 295 K are less than 0.3%.[26] These results indicate that the large MR effect in the dilute magnetic semiconductors stems from the carrier scattering due to the fluctuations and clustering of the Mn ions at or near the junction. However, for the non-magnetic silicon-based p–n junction, a large MR effect with a $\cos^2$ dependence on the angle between the current and magnetic field can be attributed to the Lorentz force.

In addition, in order to check the other possible mechanisms of anisotropic MR in the p–n junction, such as anisotropy of the Fermi surface,[28] anisotropy of orbit,[10] and geometric anisotropy,[29] *etc.*, we also carefully rotated the magnetic field in the x–z plane and x–y plane to measure the anisotropic MR effect (see the ESI†). For the x–z plane, similar results were observed, whilst for x–y plane there is no obvious anisotropic MR effect as the magnetic field is always perpendicular to the measured current. This further indicates the anisotropy MR effect in the p–n junction is mainly related to the Lorentz force that depends on the current and magnetic field orientation.

Obviously, eqn (1) was found to be successful in fitting all data over a wide range of magnetic field and current level. This allowed us to extract the $V_0(I,H)$ and $\Delta V(I,H)$ for each current and magnetic field. Fig. 5 shows the magnetic field and current dependence of the $V_0(I, H)$ and $\Delta V(I, H)$. As shown in Fig. 5a and b, V_0 is almost independent of the magnetic field H, but strongly related to the current. A similar Shockley equation of the idealized p–n junction can well describe the data in Fig. 5b, demonstrating that the transport behavior of the p–n junction is dominated by the space charge region. The weak magnetic field response for V_0 indicates that the anisotropic MR effect of the p–n junction is mainly caused by ΔV, which is angularly-dependent and strongly depends on both applied current I and magnetic field H. Fig. 5c shows that ΔV has a parabolic external magnetic field dependence, which is also consistent with the measured MR curves, as shown in the inset of Fig. 5c. Note that the MR behavior in the p–n junction that is related to H^2 differs

from that in the single doped silicon, which has a linear relationship with H due to the inhomogeneous MR effect.[10] In Fig. 5d, we plot ΔV as a function of the current for various magnetic fields. For a fixed magnetic field, the behavior can also be fitted by the Shockley equation, but as the space charge region becomes narrower at the higher current levels, ΔV is drastically enhanced, demonstrating the modulation of space charge region by the electric field. In another view, for a specific current, ΔV also increases with the increase of the magnetic field H, demonstrating the modulation of space charge region by the magnetic field.

4 Conclusions

We report a novel anisotropic MR effect in a non-magnetic p–n junction by manipulating the space charge region with the magnetic field. This anisotropic MR behavior under a wide range of current and magnetic field can be fitted well by $\sin^2(\theta)$. The analysis based on the fitted parameters reveals that the MR effect stems from the geometry changes of the space charge region induced by the magnetic field. Because this anisotropic MR effect of the silicon-based p–n junction not only has the same behavior as that in magnetic materials, but also the magnetic ratio is one order of magnitude larger than that in magnetic materials, this novel anisotropic MR could open a new way for the development of future magnetic sensors with non-magnetic materials based on p–n junctions.

Acknowledgements

This work is supported by National Basic Research Program of China (grant no. 2012CB933101), the National Natural Science Foundation of China (grant nos 50925103, 11034004, 11104122, 51372107, 51201081), Gansu Province Science and Technology Funding (grant nos 2011GS04131, 1208RJYA007 and 1208RJYA008), the Program for Changjiang Scholars and Innovative Research Team in University (grant no. IRT1251), and the Fundamental Research Funds for the Central Universities (grant no. 2022013zrct01).

References

1 H. Ohno, *Science*, 2001, **291**, 840–841.
2 R. Xu, A. Husmann, T. F. Rosenbaum, M. L. Saboungi, J. E. Enderby and P. B. Littlewood, *Nature*, 1997, **390**, 57–60.
3 J. S. Hu, T. F. Rosenbaum and J. B. Betts, *Phys. Rev. Lett.*, 2005, **95**, 186603.
4 Z. G. Sun, M. Mizuguchi, T. Manago and H. Akinaga, *Appl. Phys. Lett.*, 2004, **85**, 5643–5645.
5 S. A. Solin, T. Thio, D. R. Hines and J. J. Heremans, *Science*, 2000, **289**, 1530–1532.
6 R. Jansen, S. P. Dash, S. Sharma and B. C. Min, *Nat. Mater.*, 2012, **11**, 400–408.
7 J. J. H. M. Schoonus, P. P. J. Haazen, H. J. M. Swagten and B. Koopmans, *J. Phys. D: Appl. Phys.*, 2009, **42**, 185011.
8 J. J. H. M. Schoonus, F. L. Bloom, W. Wagemans, H. J. M. Swagten and B. Koopmans, *Phys. Rev. Lett.*, 2008, **100**, 127202.
9 M. P. Delmo, S. Kasai, K. Kobayashi and T. Ono, *Appl. Phys. Lett.*, 2009, **95**, 132106.
10 M. P. Delmo, S. Yamamoto, S. Kasai, T. Ono and K. Kobayashi, *Nature*, 2009, **457**, 1112–1116.
11 C. H. Wan, X. Z. Zhang, X. L. Gao, J. M. Wang and X. Y. Tan, *Nature*, 2011, **477**, 304–308.
12 N. A. Porter and C. H. Marrows, *Sci. Rep.*, 2012, **2**, 565.
13 S. A. Wolf, D. D. Awschalom, R. A. Buhrman, J. M. Daughton, S. von Molnar, M. L. Roukes, A. Y. Chtchelkanova and D. M. Treger, *Science*, 2001, **294**, 1488–1495.
14 M. M. Parish and P. B. Littlewood, *Nature*, 2003, **426**, 162–165.
15 M. M. Parish and P. B. Littlewood, *Phys. Rev. B: Condens. Matter Mater. Phys.*, 2005, **72**, 094417.
16 J. Hu, M. M. Parish and T. F. Rosenbaum, *Phys. Rev. B: Condens. Matter Mater. Phys.*, 2007, **75**, 214203.
17 R. Magier and D. J. Bergman, *Phys. Rev. B: Condens. Matter Mater. Phys.*, 2006, **74**, 094423.
18 V. Guttal and D. Stroud, *Phys. Rev. B: Condens. Matter Mater. Phys.*, 2005, **71**, 201304.
19 M. P. Delmo, E. Shikoh, T. Shinjo and M. Shiraish, *Phys. Rev. B: Condens. Matter Mater. Phys.*, 2013, **87**, 245301.
20 J. Luo, P. Li, S. Zhang, H. Sun, H. P. Yang and Y. G. Zhao, *Nature*, 2013, **501**, E1.
21 D. Z. Yang, F. C. Wang, Y. Ren, Y. L. Zuo, Y. Peng, S. M. Zhou and D. S. Xue, *Adv. Funct. Mater.*, 2013, **23**, 2918–2923.
22 S. Joo, T. Kim, S. H. Shin, J. Y. Lim, J. Hong, J. D. Song, J. Chang, H. W. Lee, K. Rhie, S. H. Han, K. H. Shin and M. Johnson, *Nature*, 2013, **494**, 72–76.
23 T. R. McGuire and R. I. Potter, *IEEE Trans. Magn.*, 1975, **11**, 1018.
24 D. R. Baker and J. P. Heremans, *Phys. Rev. B: Condens. Matter Mater. Phys.*, 1999, **59**, 13927.
25 S. J. May and B. W. Wessels, *Appl. Phys. Lett.*, 2006, **88**, 072105.
26 S. J. May and B. W. Wessels, *J. Vac. Sci. Technol., B: Microelectron. Nanometer Struct.–Process., Meas., Phenom.*, 2005, **23**, 1769–1772.
27 J. A. Peters, N. D. Parashar, N. Rangaraju and B. W. Wessels, *Phys. Rev. B: Condens. Matter Mater. Phys.*, 2010, **82**, 205207.
28 Z. W. Zhu, A. Collaudin, B. Fauqué, W. Kang and K. Behnia, *Nat. Phys.*, 2011, **8**, 89–94.
29 Z. J. Yue, I. Levchenko, S. Kumar, D. H. Seo, X. L. Wang, S. X. Dou and K. K. Ostrikov, *Nanoscale*, 2013, **5**, 9283–9288.